

A New Scientific Study towards Distinction of ECG Signals of a Normal healthy person and of a Congestive Heart Failure Patient

Sayan Mukherjee

Department of Mathematics, Shivanath Shastri College
23/49 Gariahat Road, Kolkata-700029, India
E-mail: msayan80@gmail.com

Sanjay Kumar Palit

Department of Mathematics
Calcutta Institute of Engineering and Management
24/1A Chandi Ghosh Road, Kolkata-700040, India

(Received December 22, 2010)

Abstract: First of all, ECG signals of healthy persons and of Congestive heart failure patients are collected from MIT-BIH database in Physionet. Next the data are tested for non-stationarity by QQ-plot method and for nonlinearity by surrogate hypothesis test. Being sure about the nonlinearity of the signals we next test for positive Lyapunov exponents prior to three dimensional attractor reconstruction of the signals. Now to reconstruct the attractors we find out proper time delay by a standard nonlinear method and then its proper embedding dimension. It is found that in all cases the embedding dimensions exceed three. Also the attractors thus reconstructed are not at all well formed. So they are not fit for the purpose of differentiation. Therefore we try for getting proper time delay under our newly developed method of generalized auto-correlation with same and different time-delays. In these cases also the embedding dimensions are found to be larger than three. Also in almost all cases the attractors are not still well formed. In fact, the three dimensional attractors are seldom well formed, as the embedding dimensions are always greater than three. However for geometrical clarity we like to stick to three dimensional attractors only. So question of distinction of the signals through their reconstructed three dimensional attractors does not arise. Thus time domain analysis to differentiate the signals in three dimensions fails. Therefore, we try for a new approach of analyzing the signals in the frequency domain in the form of 'frequency-delay plot' and its quantification. The analysis is completely new and is different from the standard periodogram analysis in the frequency domain. In frequency delay plots it is found that for normal persons the plots are really well formed and prominent too, under both cases of same delay and different delays. For Congestive heart failure patients the plots are, no doubt, so

prominent but they maintain the basic feature of being dense. So these are also workable for the purpose of differentiation. In fact, the frequency-delay plots for both categories of persons are easily differentiable visually. So we try for scientific confirmation of the differences of the plots in the two categories of persons. For this purpose, we develop a new concept of three dimensional quantification procedure, known as 'ellipsoid fit' in a three dimensional cluster. It is found that the lengths of the axes of the ellipsoids taken together behave as proper quantifying parameters, as they differ significantly in the two cases. But the results do not differ significantly if only the lengths of SD_1 and SD_2 are considered. Hence the main role of the parameters is played by the axis SD_3 only. This establishes that for proper distinction of the signals, three dimensional 'frequency-delay plots' and their quantifications are essential. No significant result can be achieved from two dimensional considerations only.

Keywords: ECG signal, Average mutual information, Generalized auto-correlation, Reconstructed attractor, Frequency-delay plot, Ellipsoid fit.

1. Introduction

The study of a continuous signal in time domain is mainly concentrated to its attractor reconstruction¹⁻¹⁰ with suitable time-delay¹¹ and to find out proper embedding dimension⁸. If the main problem is to make interpretation of the signal out of its reconstructed attractor, then the geometric method fails if the embedding dimension is more than three. Thus for geometric visualization, if the three dimensional projections of higher dimensional attractors are taken, then it is quite likely that the projected attractors are very often found to be not well-formed at all. Even if the embedding dimension⁸ is three, and attractor is well formed, still there remains much difficulty so far as quantification of the attractor is concerned. It may be noted that the whole investigation would be simpler, had the signal been discrete. In fact in that case the whole attention could be focused only on Poincaré plot reconstruction¹²⁻¹⁷ in two and three dimensions and their proper quantifications. Basically, there is a dynamics in the points of the attractor and there is a definite rule for the points on the attractor to follow. But as Poincaré plot¹²⁻¹⁷ is just a cluster of points, so there is no dynamic rule to follow by the points of this plot. This is why the former case is much complicated and difficult to handle than the latter one. Now if the signal is continuous, its three dimensional attractor is not at all well-formed or even if it is well-formed, the interpretation of the attractor is difficult, then as such there is no way out to differentiate the signals in the time domain. An alternative way is to take FFT¹⁸⁻¹⁹ of the continuous signal so as to get a discrete form of the signal and then to try for Poincaré plot reconstruction¹²⁻¹⁷ and its quantification in two and three dimension for such a discrete signal

in the frequency domain. As this is a completely new idea, so far as frequency domain analysis is concerned, so we name such a plot in the frequency domain as a “frequency-delay plot”. In this paper we introduce such a new approach of analysis of a continuous signal in the frequency domain, especially to distinguish two types of ECG signals from normal healthy persons and Congestive heart failure patients.

2. ECG Signals of Normal Healthy Persons and Congestive Heart Failure Patients

2.1. Methodology of collecting ECG signals

The electrocardiogram signal (ECG) of the normal persons and Congestive heart failure patients are downloaded from MIT-BIH data base available in Physionet website²⁰.

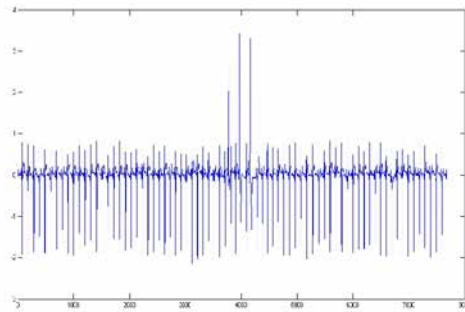


Fig.1. Time series plot of the ECG signal of a normal healthy person.

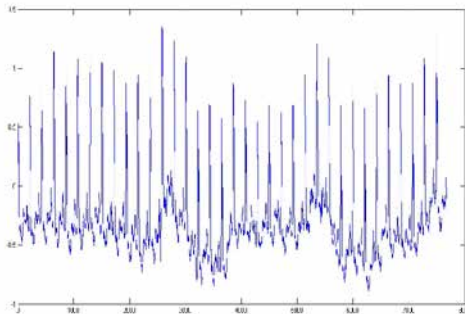


Fig.2. Time series plot of the ECG signal of a Congestive heartfailure patient

3. Test for Non-Stationarity of the Signals

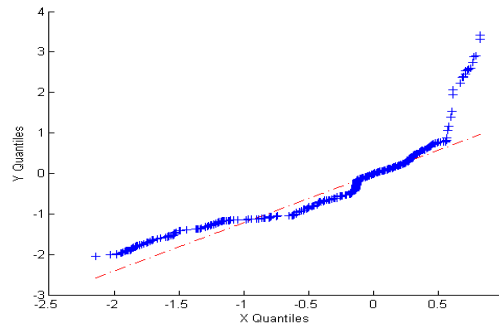


Fig.3. QQ plot of the ECG signal of a normal healthy person.

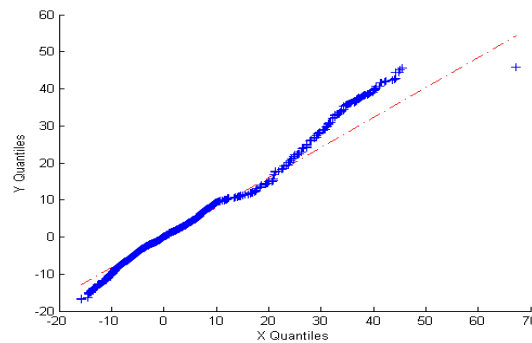
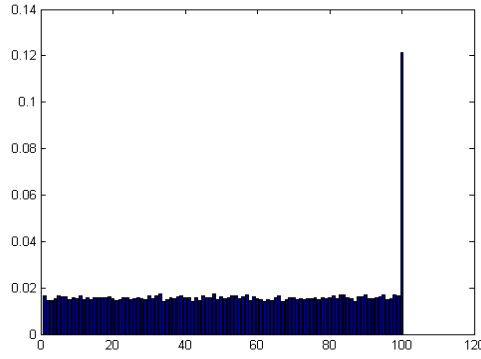
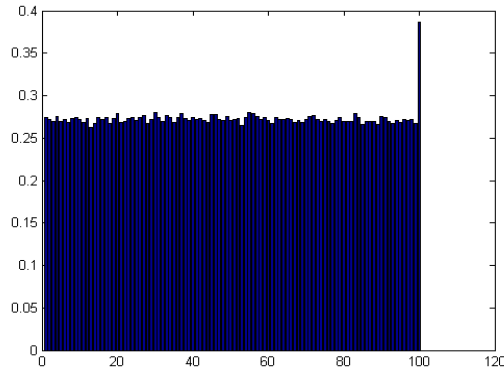


Fig.4. QQ plot of the ECG signal of a Congestive heart failure patient.

From the above QQ-plots ²¹ it is evident that in each case, the distributions are different for any two segments of equal length. This proves that the statistical parameters of the segments of equal length are always different. In other words, the signals are non-stationary.

4. Test for Nonlinearity of the Signals

The surrogate data test with 0.01 significant level ²² and the statistical parameter AMI ($\tau = 1$)(average mutual information with time-lag 1) of two ECG signals $\{x(t)\}_{k=1}^{7680}$ (for normal healthy person) and $\{y(t)\}_{k=1}^{7680}$ (for Congestive heart failure patient) are given in Fig.5. and Fig.6

Fig.5. $AMI_{normal}(\tau = 1) = AMI_{SUR(normal)}(\tau = 1)$ Figure.6. $AMI_{CHF}(\tau = 1) = AMI_{SUR(CHF)}(\tau = 1)$

In this connection, we take the null hypothesis $H_0 : AMI_{normal}(\tau = 1) = AMI_{SUR(normal)}(\tau = 1)$ (for normal healthy person) and $H_0 : AMI_{CHF}(\tau = 1) = AMI_{SUR(CHF)}(\tau = 1)$ (for Congestive heart failure patient). If the equality does not hold, we say that null hypothesis fails and alternative H_A holds good. From Fig.5 and Fig.6, it is seen that in both cases the AMI of surrogate data series is not equal to AMI of the given signal. Hence the null hypothesis $H_0 : AMI_{normal}(\tau = 1) = AMI_{SUR(normal)}(\tau = 1)$ and $H_0 : AMI_{CHF}(\tau = 1) = AMI_{SUR(CHF)}(\tau = 1)$ are rejected. Thus, nonlinearity of signals $\{x(t)\}_{k=1}^{7680}$ and $\{y(t)\}_{k=1}^{7680}$ are established through surrogate data test.

4. Reconstruction of the Attractor of the ECG Signal of a Normal Healthy Person and Congestive Heart Failure Patients

In both cases of the signals the Lyapunov exponents are found to be positive. So we try for their attractor reconstruction.

4.1. Average mutual information methods for attractor reconstruction

4.1.1. Normal healthy person

The following figures show the plot of average mutual information (AMI) ¹¹ versus time-delay τ and gives suitable delay $\tau = 8$ for attractor reconstruction.

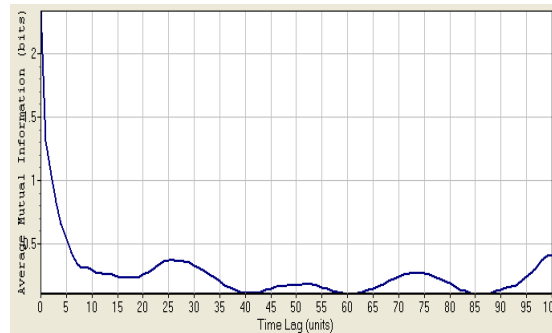


Fig. 7. Plot of Average mutual information (AMI) Vs. Time-delay.

The reconstructed attractor is given by Fig.8.

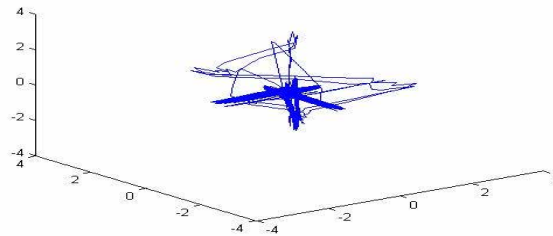


Fig.8. Reconstructed attractor of the ECG signal of the normal healthy person for $\tau = 8$

4.1.2. Congestive heart failure patient

The following fig. show the plot of average mutual information (AMI) ¹¹ versus time-delay τ and gives suitable delay $\tau = 35$ for attractor reconstruction.

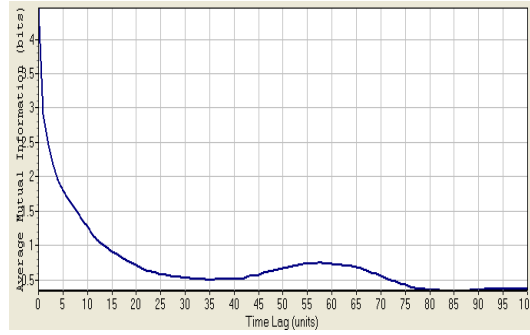


Fig. 9. Plot of Average mutual information (AMI) Vs. Time-delay

The reconstructed attractor is given by Fig.10.

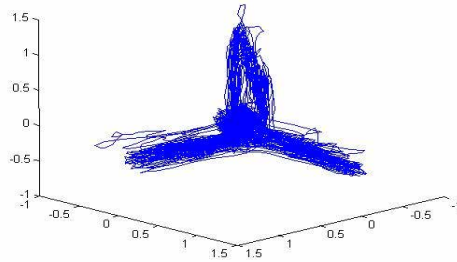


Fig.10. Reconstructed attractor of the ECG signal of a Congestive heart failure patient for $\tau = 35$.

4.1. Remark

From the Fig.8 and Fig.10, it is seen that the three dimensional attractors are not well-formed in the sense that the dense orbits are always mixed with plenty of out layers. This is quiet expected as we have verified that the embedding dimension ⁸ of attractor of ECG signal for normal healthy person is 4 and same for the Congestive heart failure patient is 8 respectively. These are much higher than three. So in this case there is no question of differentiation between the signals on the basis of their reconstructed attractors.

4.2. Generalized auto-correlation methods for attractor reconstruction

4.2.1. Generalized auto-correlation (different time-delays)

Let $\{x_1, x_2, x_3, \dots, x_N\}$ be the given time series. The generalized auto-correlation of the given time series with respect to different time-delays τ_1, τ_2 is defined by

$$(4.1) \quad R_x(\tau_1, \tau_2) = \frac{\sum_{t=1}^{N-(\tau_1+\tau_2)} \zeta_t \cdot \zeta_{t+\tau_1} \cdot \zeta_{t+\tau_1+\tau_2}}{\sqrt{\sum_{t=1}^{N-(\tau_1+\tau_2)} \zeta_t^2} \cdot \sqrt{\sum_{t=1}^{N-(\tau_1+\tau_2)} \zeta_{t+\tau_1}^2} \cdot \sqrt{\sum_{t=1}^{N-(\tau_1+\tau_2)} \zeta_{t+\tau_1+\tau_2}^2}},$$

$$\text{where } \zeta_t = (x_t - \bar{x}_t), \zeta_{t+\tau_1} = (x_{t+\tau_1} - \bar{x}_{t+\tau_1}), \zeta_{t+\tau_1+\tau_2} = (x_{t+\tau_1+\tau_2} - \bar{x}_{t+\tau_1+\tau_2}).$$

& $\tau_1, \tau_2 = 1, 2, 3, 4, \dots, (N-1)$, where \bar{x}_t , $\bar{x}_{t+\tau_1}$ and $\bar{x}_{t+\tau_1+\tau_2}$ are the means of the time series

$\{x_1, x_2, x_3, \dots, x_{N-(\tau_1+\tau_2)}\}$, $\{x_{1+\tau_1}, \dots, x_{N-\tau_2}\}$ and $\{x_{1+\tau_1+\tau_2}, \dots, x_N\}$ respectively.

4.2.1. Generalized auto-correlation (same time-delay)

In particular, when $\tau_1 = \tau_2 = \tau$, equation (4.1) reduces to

$$(4.2) \quad R_x(\tau) = \frac{\sum_{t=1}^{N-2\tau} \zeta_t \cdot \zeta_{t+\tau} \cdot \zeta_{t+2\tau}}{\sqrt{\sum_{t=1}^{N-2\tau} \zeta_t^2} \cdot \sqrt{\sum_{t=1}^{N-2\tau} \zeta_{t+\tau}^2} \cdot \sqrt{\sum_{t=1}^{N-2\tau} \zeta_{t+2\tau}^2}},$$

$$\text{where } \zeta_t = (x_t - \bar{x}_t), \zeta_{t+\tau} = (x_{t+\tau} - \bar{x}_{t+\tau}), \zeta_{t+2\tau} = (x_{t+2\tau} - \bar{x}_{t+2\tau})$$

& $\tau = 1, 2, 3, 4, \dots, (N-1)$, where \bar{x}_t , $\bar{x}_{t+\tau}$ and $\bar{x}_{t+2\tau}$ are the means of the time series $\{x_1, x_2, x_3, \dots, x_{N-2\tau}\}$, $\{x_{1+\tau}, x_2, x_3, \dots, x_{N-\tau}\}$ and $\{x_{1+2\tau}, x_2, x_3, \dots, x_N\}$ respectively.

4.2.3. Attractor reconstruction for normal healthy person (same time-delay)

The following figure shows the plot of generalized auto-correlation versus time-delay τ and gives suitable delay $\tau = 4$ for attractor reconstruction.

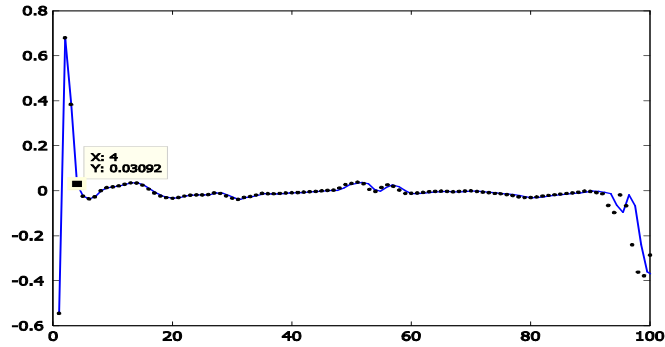


Fig. 11. Plot of Generalized auto-correlation Vs. Time-delay(X-axis)

The reconstructed attractor is given by Fig.12.

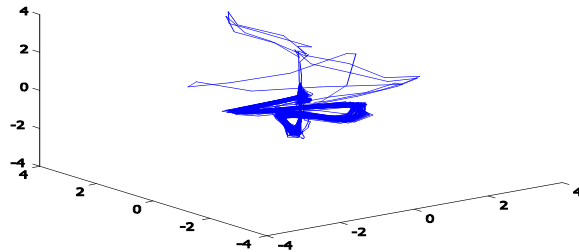


Fig.12. Three dimensional Attractor of the ECG signal of normal healthy person with $\tau = 4$ repeated.

4.2.4. Attractor reconstruction for normal healthy person (different time-delays)

The following figure shows the plot of generalized auto-correlation versus time-delays τ_1, τ_2 and gives suitable delay $\tau_1 = 1, \tau_2 = 2$ for attractor reconstruction.

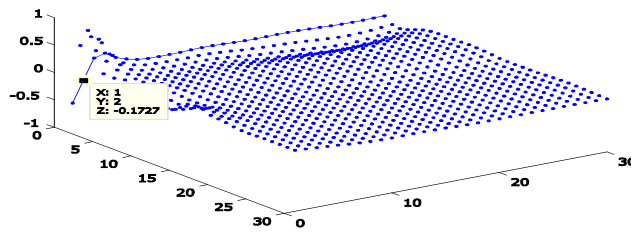


Fig.13. Three dimensional Correlogram for the ECG signal of normal healthy person under generalized auto-correlation.

The reconstructed attractor is given by Fig.14.

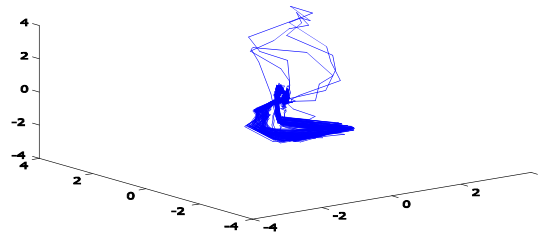


Fig.14. Three dimensional Attractor of the ECG signal of normal healthy person with $\tau_1 = 1, \tau_2 = 2$.

4.2.5. Attractor reconstruction for Congestive heart failure patient (same time-delay)

The following figure shows the plot of generalized auto-correlation versus time-delay τ and gives suitable delay $\tau = 11$ for attractor reconstruction.

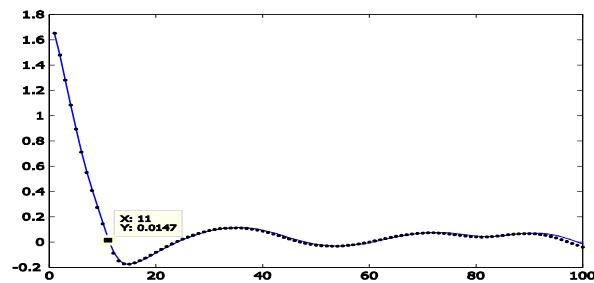


Fig. 15. Plot of Generalized auto-correlation Vs. Time-delay

The reconstructed attractor is given by Fig.16.

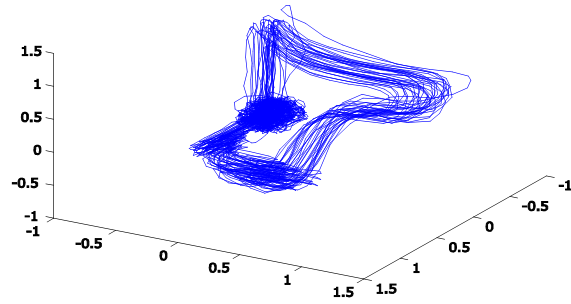


Fig.16. Three dimensional Attractor of the ECG signal of Congestive heart failure patient with $\tau = 11$ repeated.

4.2.6. Attractor reconstruction for Congestive heart failure patient (Different time-delays)

The following figure shows the plot of generalized auto-correlation versus time-delays τ_1, τ_2 and gives suitable delay $\tau_1 = 1, \tau_2 = 21$ for attractor reconstruction.

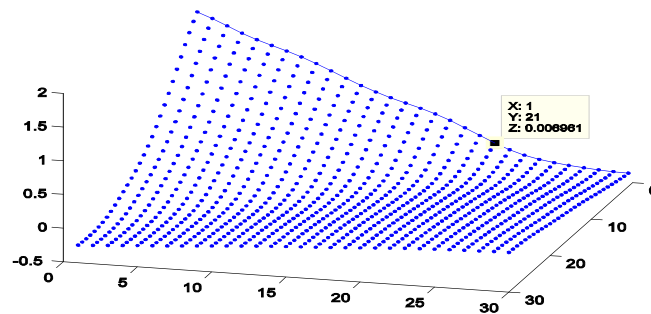


Fig.17. Three dimensional Correlogram for the ECG signal of Congestive heart failure patient under generalized auto-correlation.

The reconstructed attractor is given by Fig.18.

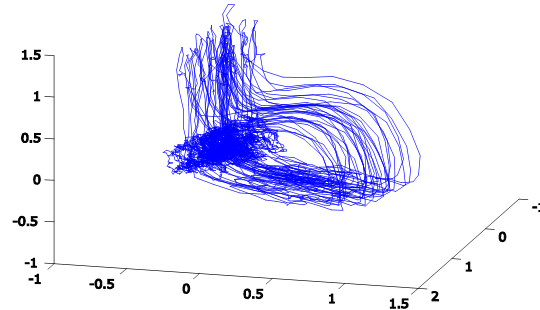


Fig.18. Three dimensional Attractor of the ECG signal of Congestive heart failure patient with $\tau_1 = 1, \tau_2 = 21$.

4.2. Remark

The concept of generalized auto correlation with same/different time-delays is newly introduced by us; it was found to produce better attractors in case of nonlinear music signals. But in the present case the Figures.12, 16, 18 are not at all of good attractors except possibly that of Figure.14. The results are not very much unexpected, as the embedding dimensions⁸ are in the present case much higher than three.

5. Frequency Domain Analysis

For the analysis of a signal in the frequency domain, very often the signal is transferred from the time domain to the frequency domain by FFT [18, 19] The transferred signal becomes fully discrete, irrespective of the given signal in the time domain, which may be discrete or continuous. It is at this point where we start our analysis by frequency-delay plot and its quantification

5.1. FFT of ECG signal of a normal healthy person and Congestive heart failure patients

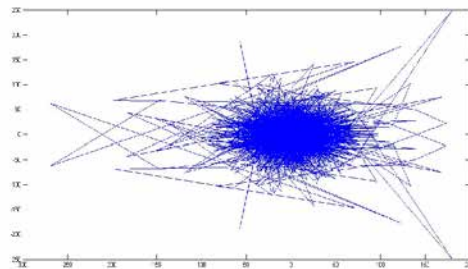


Fig.19. FFT for the ECG signal of a normal healthy person.

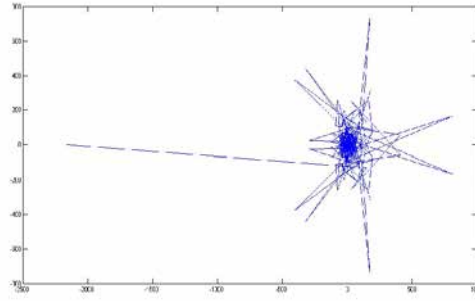


Fig. 20. FFT for the ECG signal of a Congestive heart failure patient.

The FFT ¹⁸⁻¹⁹ of the ECG signal normal healthy person and Congestive heart failure patient are given by fig.19 and fig.20 respectively.

5.2. Autocorrelation in Frequency Domain: Some New Definitions

5.2.1. Auto-correlation between two stages

Let $\{x(k)\}_{k=1}^N$ be the sample of a discrete time signal and $\{X(j) = a_j + ib_j \equiv (a_j, b_j)\}_{j=1}^N$ be its Fourier spectrum. We subdivide time series $\{X(j)\}_{j=1}^N$ into two groups $U = \{X(j)\}_{j=1}^{N-\mu} = \{(a_j, b_j)\}_{j=1}^{N-\mu}$ and $V = \{X(j)\}_{j=1+\mu}^N = \{(a_j, b_j)\}_{j=1+\mu}^N$ for delay variable $\mu = 1, 2, 3, 4, 5, \dots$. Then autocorrelation of $\{X(j)\}_{j=1}^N$ in frequency domain corresponding to delay variable μ is defined by

$$(5.1) \quad R_x(\mu) = \frac{\sum_{j=1}^N \left| \{(a_j, b_j) - (\overline{a_j}, \overline{b_j})\} \cdot \{(a_{j+\mu}, b_{j+\mu}) - (\overline{a_{j+\mu}}, \overline{b_{j+\mu}})\} \right|}{\sqrt{\sum_{j=1}^N \left| \{(a_j, b_j) - (\overline{a_j}, \overline{b_j})\} \right|^2} \cdot \sqrt{\sum_{j=1}^N \left| \{(a_{j+\mu}, b_{j+\mu}) - (\overline{a_{j+\mu}}, \overline{b_{j+\mu}})\} \right|^2}}$$

$[\mu = 1, 2, 3, 4, 5, \dots, (N-1)]$, where $(\overline{a_j}, \overline{b_j})$, $(\overline{a_{j+\mu}}, \overline{b_{j+\mu}})$ are the means of $\{(a_j, b_j)\}_{j=1}^{N-\mu}$ and $\{(a_j, b_j)\}_{j=1+\mu}^N$ respectively and $(a_r, b_r) \cdot (a_s, b_s) = (a_r a_s - b_r b_s, a_r b_s + b_r a_s)$ for $r, s = 1, 2, \dots, N$.

5.2.2. Auto-correlation amongst three stages

Let $\{x(k)\}_{k=1}^N$ be the sample of a discrete time signal and $\{X(j)=a_j+ib_j \equiv (a_j, b_j)\}_{j=1}^N$ be its Fourier spectrum. We subdivide time series $\{X(j)\}_{j=1}^N$ into three groups, $U = \{X(j)\}_{j=1}^{N-(\mu_1+\mu_2)} = \{(a_j, b_j)\}_{j=1}^{N-(\mu_1+\mu_2)}$, $V = \{X(j)\}_{j=1+\mu_1}^{N-\mu_2} = \{(a_j, b_j)\}_{j=1+\mu_1}^{N-\mu_2}$ and $W = \{X(j)\}_{j=1+\mu_1+\mu_2}^N = \{(a_j, b_j)\}_{j=1+\mu_1+\mu_2}^N$. The autocorrelation of $\{X(j)\}_{j=1}^N$ in frequency domain corresponding to delays μ_1, μ_2 is defined by

$$(5.2) \quad R_X(\mu_1, \mu_2) = \frac{\sum_{j=1}^N |\zeta_j \cdot \zeta_{j+\mu_1} \cdot \zeta_{j+\mu_1+\mu_2}|}{\sqrt{\sum_{j=1}^N |\zeta_j|^2} \cdot \sqrt{\sum_{j=1}^N |\zeta_{j+\mu_1}|^2} \cdot \sqrt{\sum_{j=1}^N |\zeta_{j+\mu_1+\mu_2}|^2}},$$

$[\mu_1, \mu_2 = 1, 2, \dots, (N-1)]$, where $\zeta_j = \{(a_j, b_j) - (\overline{a_j}, \overline{b_j})\}$,

$\zeta_{j+\mu_1} = \{(a_{j+\mu_1}, b_{j+\mu_1}) - (\overline{a_{j+\mu_1}}, \overline{b_{j+\mu_1}})\}$

and $\zeta_{j+\mu_1+\mu_2} = \{(a_{j+\mu_1+\mu_2}, b_{j+\mu_1+\mu_2}) - (\overline{a_{j+\mu_1+\mu_2}}, \overline{b_{j+\mu_1+\mu_2}})\}$.

5.3. Frequency-delay plot reconstruction of the ECG signal of a normal healthy person in frequency domain

5.3.1. Same frequency- delay repeated

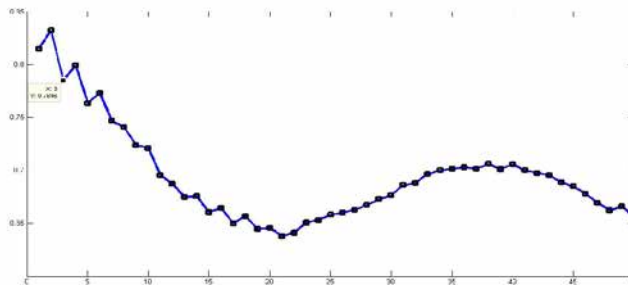


Fig. 21. Two dimensional correlogram diagram for ECG signal of a healthy person.

The reconstructed frequency-delay plot is given by Fig.22.

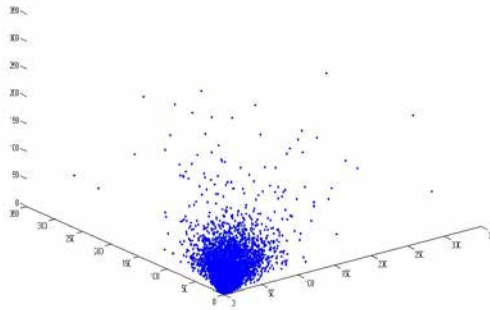


Fig. 22. Three dimensional frequency-delay plot for ECG signal of a normal healthy person with same frequency-delay.

The above figures show the two dimensional correlogram diagram and gives suitable frequency-delay $\mu = 3$ for frequency-delay plot reconstruction.

5.3.2. Different frequency-delays

The following figures show the three dimensional correlogram diagram and gives suitable frequency-delays $\mu_1 = 2, \mu_2 = 4$ for frequency-delay plot reconstruction.

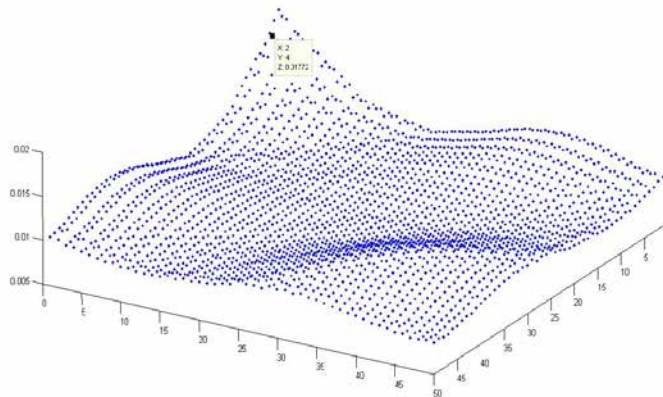


Fig.23. Three dimensional correlogram diagram for the ECG signal of a healthy person.

The reconstructed frequency-delay plot is given by Fig.24.

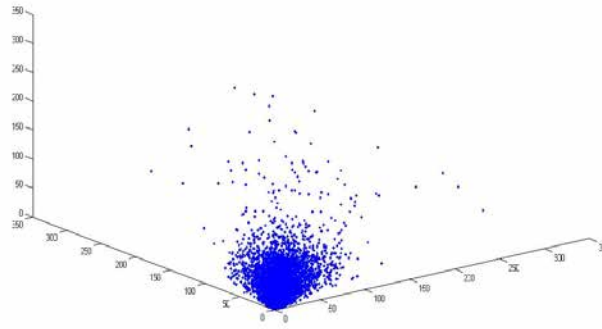


Fig.24. Three dimensional frequency-delay plot for the ECG signal of normal healthy person with different frequency –delays.

5.4. Frequency-delay plot reconstruction of the ECG signal of a Congestive heart failure patient in frequency domain

5.4.1. Same frequency- delay repeated

The following figures show the two dimensional correlogram diagram and gives suitable frequency-delay $\mu = 4$ for frequency-delay plot reconstruction.

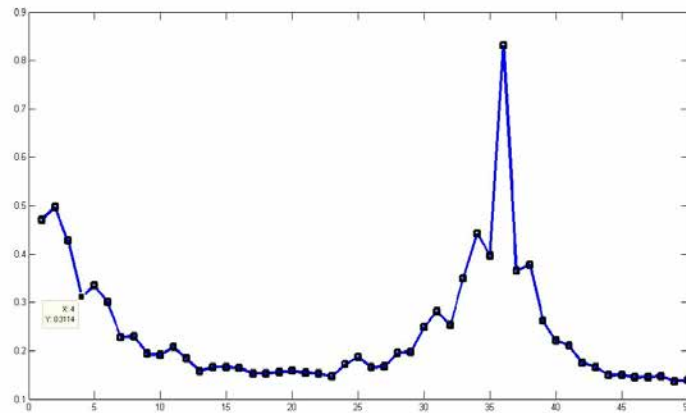


Fig.25. Two dimensional correlogram diagram for Congestive heart failure patient.

The reconstructed frequency-delay plot is given by Fig.26.

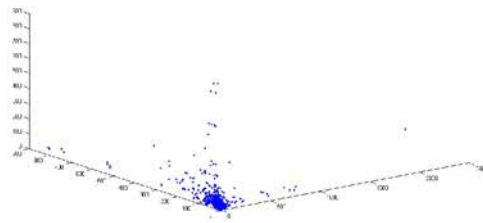


Fig.26. Three dimensional frequency-delay plot for Congestive heart failure patient with same frequency -delay.

5.4.2. Different frequency-delays

The following figures show the three dimensional correlogram diagram and gives suitable frequency-delays $\mu_1 = 1, \mu_2 = 6$ for frequency-delay plot reconstruction.

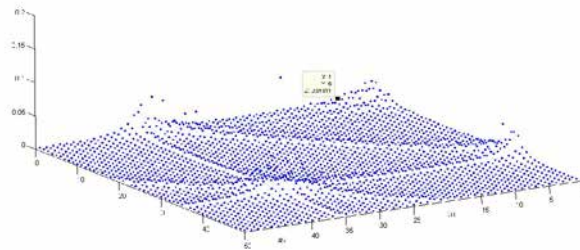


Fig.27. Three dimensional correlogram diagram for the ECG signal of Congestive heart failure patient.

The reconstructed frequency-delay plot is given by Fig.28.

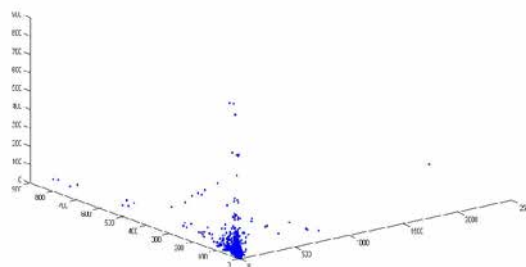


Fig.28. Three dimensional frequency-delay plot for Congestive heart failure patient with different frequency delays.

5.1. Remark

In frequency delay plots it is found that for normal healthy persons the plots are really well formed and prominent too, under both cases of same delay and different delays. For Congestive heart failure patients the plots are, no doubt, so prominent but they maintain the basic feature of being dense. So these are also workable for the purpose of differentiation. In fact, the frequency-delay plots for both categories of persons are easily differentiable visually. So we try to account for such differences more scientifically.

5.5. Frequency-delay clustering in three dimensions

Frequency-delay clustering in three dimensions is a newly proposed quantification technique, which is used to distinguish two different frequency-delay plots in three dimensions. In this section, we first extend the notion of frequency-delay Clustering in two dimensions for any discrete signal $\{x(k)\}_{k=1}^N$ with same delay. Next we generalize it for any discrete signal $\{x(k)\}_{k=1}^N$ with different delays. Finally, we apply this technique to differentiate the three dimensional frequency-delay plots in frequency domain for the aforesaid ECG signal of the normal healthy person and that of the patient with Congestive heart failure by their proper quantifications.

5.5.1. Frequency-delay clustering with same delay

Let $\{x(k)\}_{k=1}^N$ be a discrete signal. Let that the three dimensional frequency-delay plot be constructed by sub-dividing this signal into three groups as x^+, x^-, x^{--} with same delay τ , where

$$x^+ = \{x(k)\}_{k=1}^{N-2\tau}, \quad x^- = \{x(k)\}_{k=1+\tau}^{N-\tau}, \quad x^{--} = \{x(k)\}_{k=1+2\tau}^N, \quad \tau = 1, 2, \dots, (N-1).$$

We transform this co-ordinate system by a three dimensional rotation with same angle $\frac{\pi}{4}$ with respect to X, Y and Z axis. The transform is given by

$$\begin{pmatrix} x_m \\ x_n \\ x_p \end{pmatrix} = \begin{pmatrix} \cos \frac{\pi}{4} \cos \frac{\pi}{4} & \cos \frac{\pi}{4} \sin \frac{\pi}{4} \sin \frac{\pi}{4} - \cos \frac{\pi}{4} \sin \frac{\pi}{4} & \cos \frac{\pi}{4} \cos \frac{\pi}{4} \sin \frac{\pi}{4} + \sin \frac{\pi}{4} \sin \frac{\pi}{4} \\ \cos \frac{\pi}{4} \sin \frac{\pi}{4} & \cos \frac{\pi}{4} \cos \frac{\pi}{4} + \sin \frac{\pi}{4} \sin \frac{\pi}{4} \sin \frac{\pi}{4} & -\cos \frac{\pi}{4} \sin \frac{\pi}{4} + \cos \frac{\pi}{4} \sin \frac{\pi}{4} \sin \frac{\pi}{4} \\ -\sin \frac{\pi}{4} & \cos \frac{\pi}{4} \sin \frac{\pi}{4} & \cos \frac{\pi}{4} \cos \frac{\pi}{4} \end{pmatrix} \begin{pmatrix} x^+ \\ x^- \\ x^{--} \end{pmatrix}$$

$$= \frac{1}{2\sqrt{2}} \begin{pmatrix} 2\sqrt{2} & -(\sqrt{2}-1) & (\sqrt{2}+1) \\ 2\sqrt{2} & (\sqrt{2}+1) & -(\sqrt{2}-1) \\ -2 & \sqrt{2} & \sqrt{2} \end{pmatrix} \begin{pmatrix} x^+ \\ x^- \\ x^{--} \end{pmatrix}.$$

Hence,

$$\begin{aligned} x_m &= \frac{1}{2} \cdot x^+ + \left(\frac{1}{2\sqrt{2}} - \frac{1}{2}\right) \cdot x^- + \left(\frac{1}{2\sqrt{2}} + \frac{1}{2}\right) \cdot x^{--} = \frac{2\sqrt{2} \cdot x^+ - (\sqrt{2}-1) \cdot x^- + (\sqrt{2}+1) \cdot x^{--}}{2\sqrt{2}}; \\ x_n &= \frac{1}{2} \cdot x^+ + \left(\frac{1}{2\sqrt{2}} + \frac{1}{2}\right) \cdot x^- + \left(\frac{1}{2\sqrt{2}} - \frac{1}{2}\right) \cdot x^{--} = \frac{2\sqrt{2} \cdot x^+ + (\sqrt{2}+1) \cdot x^- - (\sqrt{2}-1) \cdot x^{--}}{2\sqrt{2}}; \\ x_p &= \left(-\frac{1}{\sqrt{2}}\right) \cdot x^+ + \frac{1}{2} \cdot x^- + \frac{1}{2} \cdot x^{--} = \frac{-2 \cdot x^+ + \sqrt{2} \cdot x^- + \sqrt{2} \cdot x^{--}}{2\sqrt{2}}. \end{aligned}$$

Thus a new co-ordinate system (x_m, x_n, x_p) is formed.

Let $\bar{x}_m = \text{Mean}(x_m)$, $\bar{x}_n = \text{Mean}(x_n)$, $\bar{x}_p = \text{Mean}(x_p)$ and $SD_1 = \sqrt{\text{Var}(x_m)}$, $SD_2 = \sqrt{\text{Var}(x_n)}$, $SD_3 = \sqrt{\text{Var}(x_p)}$. Lastly, an ellipsoid centered at $(\bar{x}_m, \bar{x}_n, \bar{x}_p)$ with three axes of length SD_1 , SD_2 and SD_3 is taken for quantification of existing frequency-delay plot. In fact, SD_1 , SD_2 and SD_3 are the quantifying parameters for the frequency-delay clustering in three dimensions.

5.5.2. Frequency-delay clustering with different delays

To generalize the above notion for discrete signal $\{x(k)\}_{k=1}^N$ with different delays τ_1, τ_2 , we just change the sub-division of the signal as follows:

$x^+ = \{x(k)\}_{k=1}^{N-(\tau_1+\tau_2)}$, $x^- = \{x(k)\}_{k=1+\tau_1}^{N-\tau_2}$, $x^{--} = \{x(k)\}_{k=1+\tau_1+\tau_2}^N$, where $\tau_1, \tau_2 = 1, 2, \dots, (N-1)$ and proceed as before to get the parameters of quantification for frequency-delay clustering in three dimensions.

5.5.3. Application of the technique of frequency delay plot in three dimensions

We now use the above technique to quantify the frequency-delay plot for the ECG signals of normal healthy person and that of Congestive heart failure patient. This is summarized in the following table:

Quantification Table

ECG Signals	SD_1	SD_2	SD_3
Normal healthy person (same frequency-delay)	34.6443	34.9380	15.0340
Normal healthy person (different frequency –delays)	33.9765	35.7254	14.7903
Congestive heart failure patient (same frequency-delay)	47.3807	48.8332	29.8604
Congestive heart failure patient (different frequency delays)	48.3596	52.5946	26.4572

Table.1. SD_1 , SD_2 and SD_3 of the frequency-delay plot for ECG signals of normal healthy person and Congestive heart failure patients.

6. Result and Discussion

- (a) In time domain analysis a major query is to see whether the time series is of chaotic nature. Naturally attractor reconstruction¹⁻¹⁰ is the primary investigation. But if there are two such time series and the problem is to differentiate them, then it is not so easy to make a distinction on the basis of only the two attractors reconstructed. But if the frequency-delay plots in frequency domain are considered, then through their quantification parameters it can be done in an easier and more rigorous way.
- (b) Actually it has been possible to identify the signal of a normal healthy person from that of a Congestive heart failure patient by frequency delay plot.
- (c) The results have been obtained on the basis of the signals taken from each of 50 normal healthy persons and 50 Congestive heart failure patients. For definiteness, the results are shown based on the data of one normal healthy person and one Congestive heart failure patient only.

References

1. D. T. Kaplan and L. Glass, *Understanding Nonlinear Dynamics*, Springer, New York, 1995.
2. H. D. I. Abarbanel, *Analysis of Observed Chaotic Data*, Springer-Verlag, New-York, 1997.
3. D. T. Kaplan, *Signal Processing, war wick- exercises. tex.*, **5** 2004.
4. D. J. Christini, F. M. Bennett, K. R. Lutchen, H. M. Ahmed, J. M. Hausdorff and N. Oriol, *IEEE Trans. Biomed. Eng.* **42** (1995) 411.
5. J. P. Eckmann and D. Ruelle, Ergodic theory of chaos and strange attractors, *Rev. Mod.Phys.*, **57** (1985) 617.

6. L. Glass and M. C. Mackey, *From clocks to chaos: the rhythms of life*, Princeton, NJ: Princeton University Press, 1988.
7. F. Takens, *In Dynamical systems and turbulence*. **898** (1981) 366.
8. E. Ott, *Chaos in dynamical systems*, Cambridge University Press, Cambridge, 1993.
9. D. Ruelle, *Chaotic Evolution and Strange Attractors*, Cambridge University Press, Cambridge, 1989.
10. Frank GW, Look man T, N. Mah and C. Essex, Chaotic time series analyses of epileptic seizures, *Physica D.*, **46** (1990), pp. 427.
11. G. P. Williams, *Chaos Theory Tamed*, Joseph Henry Press, Washington, D.C., 1997.
12. J. Piskorski, Filtering Poincaré plots, *Computational Methods in Sc & Tech.*, **11** (2005) 39.
13. M. Brennan, M. Palaniswami and P. Kamen, Do existing measures of Poincaré plot geometry reflect nonlinear features of heart rate variability? *IEEE Trans. Biomed. Eng.*, **48** (2001) 1342.
14. J. Haaksma, J. Brouwer , W.A. Dijk, W.R.M. Dassen and D.J.V. Veldhuisen, Applicability and performance of heart rate variability methods, *IEEE Trans. Comp. in Cardiol.*, **29** (2003) 453.
15. H. Otzenberger, C. Simon, C. Gronfier and G. Brandenberger, Temporal relationship between dynamic heart rate variability and electroencephalographic activity during sleep in man, *Neuroscience Letters.*, **229** (1997) 173-176.
16. S Mensing, J Limberis, G Gintant, A Safer, A Novel Method for Poincaré Plot Shape Quantification Demonstrates Cardiac Tissue Repolarization Inhomogeneities Induced by Drugs, *Computers in Cardiology.*, **35** (2008) 18.
17. A. Voss, S. Schulz, R. Schroeder, M. Baumert and P. Caminal , Methods derived from nonlinear dynamics for analysing heart rate variability, *Phil Trans. R Soc. A* (2009) 277-296.
18. L. C. Andrews, B. K. Shivamoggi, *Integral Transforms for Engineers* , Prentice-Hall of India, 2005.
19. M. Weeks, *Digital Signal Processing*, Infinity Science Press LLC, Hingham, Massachusetts, 2007.
20. W. L. Martinez and A. R. Martinez, *Computational Statistics Handbook with Matlab*, Chapman & Hall/CRC, 2002.
21. D. L. Guarín L'opeza, A. A.O. Gutierrez and E. D. Trejos, A new surrogate data method for nonstationary time series, *Nonlinear Analysis: Real World Applications*, 2010.